

1 Article

# 2 *Ab initio* molecular dynamics simulation of 3 tribochemical reactions involving phosphorus 4 additives at sliding iron interfaces

5 S. Loehlé,<sup>1</sup> and M. C. Righi<sup>2,3\*</sup>

6 <sup>1</sup> Total Marketing and Services, Chemin du Canal BP 22, 69360 Solaize, France

7 <sup>2</sup> Department of Physics, Informatics and Mathematics, University of Modena and Reggio Emilia, Via Campi  
8 213/a 41124 Modena, Italy

9 <sup>3</sup> CNR INStitute od Nanoscience, , Via Campi 213/a 41124 Modena, Italy

10

11 \* Correspondence: mcrighi@unimore.it; Tel.: +39-059-2055334

12

13 **Abstract:** We performed for the first time to our knowledge fully *ab initio* molecular dynamics  
14 simulations of additive tribochemistry in boundary lubrication conditions. We consider an  
15 organophosphorus additive that has been experimentally shown to reduce friction in  
16 steel-on-steel sliding contacts thanks to the tribologically-induced formation of an iron phosphide  
17 tribofilm. The simulations allow us to observe in real time the molecular dissociation at the sliding  
18 iron interface under pressure and to understand the mechanism of iron phosphide formation. We  
19 discuss the role played by the mechanical stress by comparing the activation times for molecular  
20 dissociation observed in the tribological simulations at different applied loads with that expected  
21 on the basis of the dissociation barrier.

22 **Keywords:** lubricant additives; boundary lubrication; *ab initio* molecular dynamics; tribochemistry;  
23 organophosphorus additives

24

## 25 1. Introduction

26 The technologies nowadays available to reduce friction and wear are based on materials, an  
27 important class of which is represented by lubricant additives included in motor oils. The design of  
28 lubricant additives to decrease friction and wear in machine components is an important way to  
29 increase the energy efficiency of car engines while taking into account restrictive environmental  
30 requirements and technological advances.[1] Lubricants are formulated products composed of base  
31 oil and a package of additives designed for specific performance needs. The additives can be  
32 classified as chemically active, i.e., designed to chemically interact with the surface and form  
33 protective layers, or chemically inert, i.e., with the function of improving the physical properties of  
34 the base oil. Most of the chemically active additives have a non-polar part, usually consisting of a  
35 hydrocarbon chains that solubilize the molecule into the base oil, and a functional polar group that is  
36 tailored for the specific function that the additive should carry out. Here we consider  
37 extreme-pressure (EP) additives that operate in boundary lubrication conditions, where the  
38 thickness of the oil film becomes too thin to prevent direct contact between the metal asperities. EP  
39 additives typically adsorb onto the metal surface either by physical or chemical attraction.[2,3]  
40 Under severe tribological conditions, they react with the surfaces forming surface films that prevent  
41 the welding of opposing asperities and avoid scuffing that is destructive to sliding surfaces under  
42 high loads.[4] To improve boundary lubricants is highly desirable to understand how these  
43 protective films are formed by tribochemical reactions. However, many aspects of tribochemistry  
44 remain elusive due to the difficulties in directly probing the buried interface. From post mortem  
45 spectroscopy, it is possible to acquire information on the reaction products, but very little can be  
46 inferred on the activation mechanisms, reaction pathways and rates. Simulations can play a decisive

47 role here,[5,6] in particular *ab initio* molecular dynamics (AIMD), where both the ionic and  
48 electronics degrees of freedom are fully taken into account. This is essential for an accurate  
49 description of bond-breaking and bond-forming reactions in the situation of enhanced reactivity  
50 imposed by the boundary lubrication conditions. However, the use of AIMD in tribology has been  
51 traditionally very scarce and most of the existing simulations of tribochemistry are based on force  
52 fields, i.e., on a parameterization of the atomic interactions. While many force fields are available for  
53 selected chemical environments, their transferability is often poor, especially to describe the  
54 non-ordinary conditions present at the tribological interface.

55 Here we apply AIMD to investigate tribochemistry mechanisms that govern the functionality of  
56 EP additives where the key element of the functional group is phosphorus. P-based compounds are  
57 largely used as EP and anti-wear (AW) additives for gear oils.[7-9] The chemical structure of  
58 P-containing additives influences the nature and the tribological performances of the tribofilm as  
59 highlighted in [10-12], where phosphite and phosphate have been compared. Typically, organic  
60 phosphites function as friction-modifiers whereas phosphates as AW additives.

61 A convenient experimental set up to study the tribochemistry of lubricant additives in  
62 boundary lubrication conditions is represented by gas phase lubrication (GPL), where gaseous  
63 molecules containing the same functional group of commercial additives are introduced in the  
64 tribometer chamber and react with the metallic sliding parts in contact in the absence of the base oil.  
65 Among all types of phosphite additives, trimethylphosphite (TMPi), with chemical formulae  
66  $P(CH_3O)_3$ , is probably the simplest compound containing the phosphite ion, thus it was chosen in  
67 the GPL experiments performed by Phillipon *et al.* to provide a basic understanding on the  
68 functionality of organophosphorous additives.[13-15] The experiment revealed that TMPi  
69 decomposes on nascent iron surfaces and the tribological conditions favor the formation of an iron  
70 phosphide tribofilm that significantly reduces the coefficient of friction and wear at the steel-steel  
71 sliding contact.

72 To identify the mechanisms of TMPi dissociation, we combined first principles calculation and  
73 XPS analysis of TMPi adsorption and dissociation at the open Fe(110) surface.[16] The calculated  
74 reaction energies indicate that dissociation is energetically more favorable than molecular  
75 adsorption and it is a thermally activated process. *In situ* XPS analysis of adsorbed TMPi on metallic  
76 iron confirmed molecular chemisorption and dissociation at high temperature. In the present paper  
77 the effects of tribological conditions, which include confinement, mechanical stresses (load and  
78 shear) on the reaction of TMPi dissociation are highlighted. This is accomplished by comparing the  
79 results obtained at the open surface in static conditions with AIMD imitations of TMPi molecules  
80 confined at sliding iron interfaces under load. These AIMD simulations represent a great  
81 computational challenge due to difficulty imposed by the presence of a metallic system where the  
82 ionic and electronic degrees of freedom can exchange energy due to the absence of a band gap. In  
83 addition, the magnetic character of iron imposes the use of spin polarization. We face this challenge  
84 by adopting the Born Oppenheimer (BO) scheme, where the ions are moved according to the  
85 Hellmann-Feynman forces obtained from the total electronic energy, which is minimized every MD  
86 step. In this way the ionic and electronic degrees of freedom are decoupled and the dynamics of  
87 metallic systems, even including magnetization, can be described in accurate way. The observed  
88 tribochemical reactions clarify the mechanism of P release at the buried interface, in agreement with  
89 the experimental observations and with the first-principle study of molecular decomposition at the  
90 open surface.[16] However, the observed dissociation rates are much higher in tribological  
91 conditions: By repeating the tribological AIMD simulation at different applied loads we highlight  
92 the primary role of mechanical stresses in promoting the reactions.

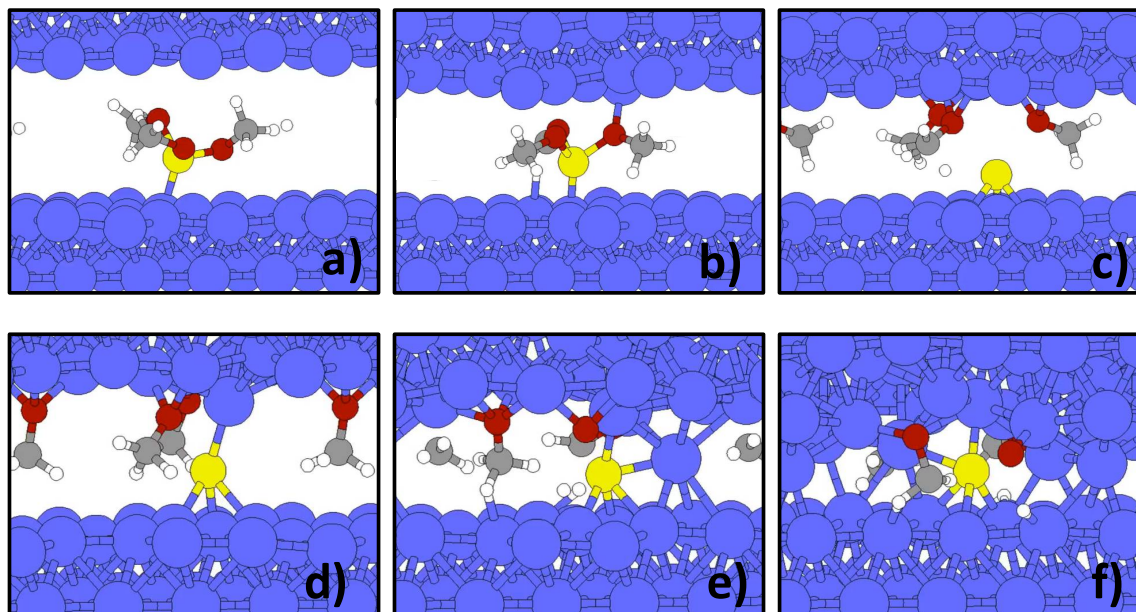
## 94 2. Materials and Methods

95 We perform spin-polarized density functional theory (DFT) calculations, using a modified  
96 version of the BO MD code included in the Quantum Espresso package.[17] The exchange  
97 correlation functional is described by the Perdew, Burke, Ernzerhof (PBE) parameterization.[18] The

98 electronic wave functions are expanded in plane-waves with kinetic energy cut-off of 30 Ry (240 Ry  
99 for the charge density). The Fe(110) surface is considered since it is the most stable among the  
100 densely packed iron surfaces.[19] The surface is modeled by means of periodic supercells containing  
101 an iron slab of (4x4) in-plane size, e.g. 16 atoms per layer, and a vacuum region 20 Å thick. It has  
102 been verified that the choice of the (4x4) in-plane size is sufficient to avoid lateral interaction of TMPi  
103 with its periodic replicas. The Brillouin zone sampling is realized by means of a (2x2x1) Monkhorst  
104 Pack grid.[20] Iron interfaces, are modeled by two self-mated Fe(110) surfaces. During the AIMD  
105 simulations the bottom layer of the lower slab (the substrate) was held rigid, while the upper slab  
106 (the counter-surface) was moved at constant velocity of 200 m/s. This velocity is much higher than  
107 the typical sliding speed in a tribometer at boundary conditions (~70 mm/s). However, the  
108 agreement between the reaction path observed in the AIMD simulation and that predicted by static  
109 first principles calculations, which are also consistent with thermal decomposition observed in  
110 experiments, make us to believe that the high sliding velocity imposed in the dynamic simulation  
111 does not alter the reaction paths of the chemical processes. In other words, the chemical processes  
112 that are most likely to occur on the basis of thermodynamics are the same observed at high sliding  
113 velocity. A vertical force was applied to the atoms belonging to the top layer of the counter- surface  
114 to model an applied pressure the value of which was varied from 500 MPa to 5 GPa to evaluate the  
115 dependence of the reaction rates on load. In the initial configuration, common to all the performed  
116 simulations, a TMPi molecule per cell (of ~100 Å<sup>2</sup> area) was adsorbed in its most stable configuration  
117 on the iron substrate and the system was relaxed under the effects of the applied pressure. After the  
118 relaxation at 500 MPa pressure, the system was equilibrated at a constant temperature of 300 K. This  
119 starting system configuration is common to all the simulations at different applied loads.  
120

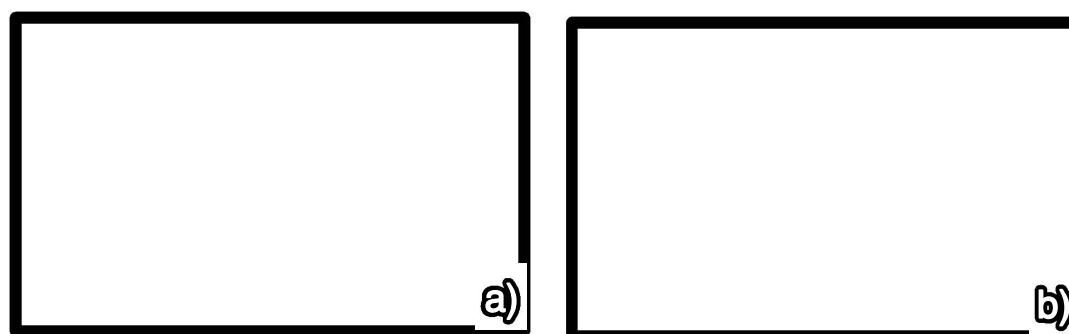
### 121 3. Results

122 The first AIMD simulation, which is carried out at 500 MPa load, is available as Video S1 in the  
123 supplemental information (SI). The system dynamics observed during a time interval of 7 ps consists  
124 in molecular vibrations, mainly rotations of each methyl group around the axis along the CO bond,  
125 and we do not observe any dissociative reaction. By increasing the pressure to 2 GPa, molecular  
126 dissociation is, instead, observed after 1 ps. As can be seen in Fig. 1a,b, the increased load makes the  
127 iron counter-surface to get closer to the substrate. This load-induced confinement promotes the  
128 molecular dissociation that occurs via PO bond breaking. As can be seen in the atom trajectory  
129 reported as Video S2, the oxygen atoms are attracted by the incoming iron counter-surface, the PO  
130 bonds get stretched and finally methoxy groups (OCH<sub>3</sub>) dissociate and adsorb on the  
131 counter-surface leaving elemental phosphorus remains on the substrate (Fig. 1c). We notice that the  
132 P atom is located at a long bridge site, which is indicated as the most favorable site for P adsorption  
133 at the Fe(110) surface by first principles calculations of adatom chemisorption.[21]



134 *Fig. 1* Snapshots acquired during AIMD simulation of TMPi tribochemistry at sliding iron interface under 2  
 135 GPa pressure and room temperature. The simulation time increases from panel (a) to panel (f). Fe is colored in  
 136 blue, P in yellow, O in red, C in grey, and H in white. The whole simulation (Video S2) is available in the SI.

137 The simulation snapshot presented in panel d) highlights the tendency of phosphorus at low  
 138 concentration to interact with the Fe counter-surface: a Fe atom not involved in FeO bonds is  
 139 “captured” by the P atom and drags downward the substrate. The surface separation is reduced and  
 140 a direct contact between few metal atoms established (Fig. 1e). It is very interesting to notice that this  
 141 direct metal-metal contact is sufficient to promote the cold sealing of the two iron surfaces. Upon  
 142 surface sealing the molecular fragments remain embedded in the iron matrix (Fig. 1f). This event in  
 143 real life would be detrimental, corresponding e.g. to engine seizure. However, we expect that the  
 144 direct metal-metal contact can be prevented by an increased phosphorous coverage. This would  
 145 explain the wear and friction reduction provided by the iron phosphide tribofilm, observed in the  
 146 experiments. In Fig. 2 we show the initial and final configurations of the optimization process at zero  
 147 applied load for an iron interface passivated with 0.5 ML (a) and 1 ML of P atoms (b). We can  
 148 observe that the interfacial P highly reduces the work of separation of iron ( $W_{\text{sep}}$  of clean iron is 4.8  
 149 J/m<sup>2</sup>). Moreover direct Fe-Fe contact is inhibited at the interface at the considered P coverages: At 0.5  
 150 ML coverage chemical Fe-P-Fe bonds are present across the interface, while at 1 ML coverage the  
 151 fully passivated surfaces repulse each-other and the Fe-Fe distance increases to 7.3 Å. The observed  
 152 adhesion reduction is accompanied by a dramatic decrease of the interfacial shear strength.[21]  
 153

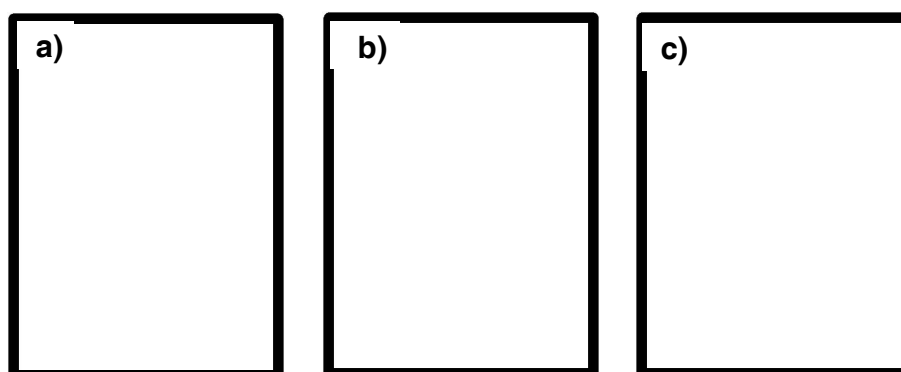


154 *Fig. 2* Initial and final configurations of the optimization process at zero applied load for an iron interface  
 155 passivated with 0.5 ML (a) and 1ML (b) of P atoms. The calculated work of separation,  $W_{\text{sep}}$ , and equilibrium  
 156 distance,  $d_{\text{Fe-Fe}}$ , are reported in each panel.

157  
158 In the AIMD simulation at the higher applied load of 5 GPa the molecular dissociation occurs  
159 following the same path as observed at 2 GPa, but the dissociation takes place just 0.6 ps after the  
160 beginning of the simulation (Video S3 of SI). This suggests that the activation rate of tribochemical  
161 reactions increases with the load applied at the sliding interface, as discussed in the next session.

162 A closer inspection of the molecular fragments embedded in the iron matrix (Fig. 1f) reveals  
163 that the methoxy groups got dissociated into H atoms on CO molecules. To identify the driving force  
164 for this process, we calculate the reaction energy,  $E_R$ , associated to methoxy dehydrogenation. First  
165 identify the most favorable adsorption sites for the  $\text{OCH}_3$  group, CO and H on the Fe(110) surface.  
166 The reaction energy is, in fact, calculated as the difference between the adsorption energy of the  
167 methoxy group and that of the adsorbed CO and H fragments. We find that the most favorable  
168 adsorption site for both methoxy and H adsorption is the three-fold site, where the adsorbates are  
169 bounded with three Fe atoms (Fig. 3a,c). The CO molecule, instead, does not chemisorb on iron:  
170 during the relaxation process the molecule detaches from the surface and remains physisorbed at 4.1  
171 Å distance from the on-top site, where physisorption is more favorable (Fig. 3b). By tilting the  
172 molecule upside-down with the C atom closer to the surface we obtain a slightly lower  
173 physisorption attraction. The calculated reaction energy for methoxy dehydrogenation is -0.87 eV.  
174 The negative sign indicates that this process is energetically favored, confirming the reliability of the  
175 AIMD simulation.

176  
177  
178  
179



180 *Fig. 3 Optimized adsorption configurations for methoxy (a), CO (b) and H (c) adsorbed on the Fe(110) surface.*  
181 *CO adsorption is modeled using a (4x4) cell, while a (2x2) cell is used both for methoxy and H adsorption. In the*  
182 *case of H, the most favorable adsorption is obtained by considering two atoms per cell, both at three-fold sites.*

183

#### 184 4. Discussion

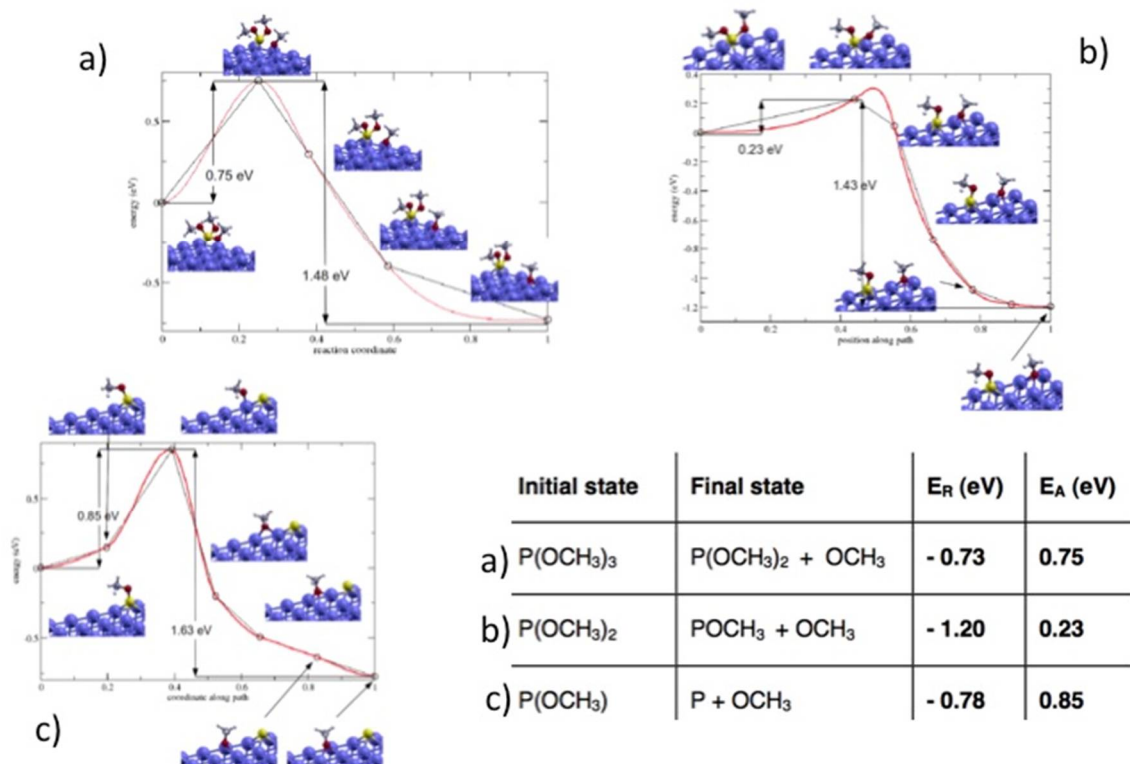
185 The reaction path observed during the AIMD simulation indicates that the molecular  
186 dissociation occurs through the cleavage of the PO bonds that cause methoxy detachment. As can be  
187 seen by comparing Fig.1a and 1b, the O atoms of the molecule are attracted by the Fe counter-surface  
188 and when the latter is close enough, the methoxy groups detach from the TMPi molecule and adsorb  
189 on it. These findings indicate that clean Fe sites are necessary for TMPi dissociation on the surface  
190 and explain the important role of the nascent surfaces in favoring the adsorption and dissociation of  
191 TMPi observed experimentally [13]. Particularly, the freshly scratched surfaces in vacuum might  
192 expose a higher number of Fe atoms than flat surfaces.

193 The decomposition path highlighted by the AIMD simulations is perfectly consistent with the  
194 decomposition path identified by combining temperature-programmed reaction spectroscopy, X-ray  
195 photoelectron spectroscopy (XPS) and low-energy electron diffraction. In this experiment, it is  
196 observed that TMPi decomposes on the clean Fe(110) into adsorbed phosphorous, gaseous CO and

197 H<sub>2</sub> via the methoxy intermediate, leaving behind a phosphide film. [22] The thermally-activated  
198 formation of iron phosphide has been also observed upon TMPi adsorption at etched steel surfaces.  
199 The characteristic peak of iron phosphide appeared clearly at a temperature of 300 °C. These results  
200 strongly suggest that the formation of iron phosphide occurs if an energy barrier is overcome.[21]

201 We estimated the height of the energy barrier for TMPi dissociation at the Fe(110) surface by  
202 first principles calculations.[21] The results obtained by applying the nudged elastic band  
203 method[23] are schematically represented in Fig. 4. The three panels describe the calculated reaction  
204 paths for the subsequent detachment of the methoxy groups, while the corresponding reaction  
205 energies and barriers are reported in the table enclosed in the picture. The negative values of E<sub>R</sub>  
206 indicate that the molecular dissociation via methoxy detachment is a highly exothermic process and  
207 the energy gain increases until the full molecular decomposition in atomic P and 3 adsorbed  
208 methoxy groups is realized. It is interesting to notice that these thermodynamical driving forces can  
209 explain the molecular dissociation observed during the dynamic simulation.

210  
211 The calculated activation barriers, E<sub>A</sub>, indicate that methoxy detachment occurs upon energy  
212 transfer, as observed in the thermal programmed experiments above described. The fact that the  
213 TMPi dissociation is observed in our AIMD simulations at *room temperature* highlights the capability  
214 of mechanical stresses to activate the reaction. Moreover, the activation time observed in the  
215 tribological simulation turned out to be much shorter than the activation time expected by applying  
216 the Arrhenius law at room temperature, considering a limiting barrier of 0.75-0.85 eV, (Tab of Fig. 4).  
217 This result, along with the trend that we observed by increasing the applied load from 500 MPa to 2  
218 and 5 GPa indicate that the load-induced confinement plays a crucial role in accelerating the reaction  
219 rates. The important role of load-induced confinement has been previously highlighted by AIMD  
220 simulations of tribochemical reactions involving water molecules confined at diamond  
221 interfaces.[24,25] In particular, it was found that the higher the load, the more effective the surface  
222 passivation by water dissociation, which in turn leads to a reduction of friction.[24] AIMD  
223 simulations offer the opportunity to isolate the effects of mechanical stresses from other effects,  
224 which have been proposed to activate tribochemical reactions. The first proposed mechanisms [26]  
225 attributed the increase of the reaction rates to extremely high temperatures, "flashes temperatures,"  
226 that develop at few discrete "hot spots," where the contact between the two surfaces occurs.[27]  
227 Such temperature increase has been also proposed to produce local excitations, "magma plasma,"  
228 that decay rapidly into a local heating of the surface.[28] However, recent works have shown that  
229 tribochemical reactions can take place even though the temperature raise during sliding is negligible  
230 or limited and highlighted the primary role of mechanical stresses in the activation of chemical  
231 reactions. [29-38]



232 **Fig. 2** Reaction paths, energies,  $E_R$ , and barriers,  $E_A$ , for the detachment of the first (a), second (b) and third (c)  
 233 methoxy group from the TMPi molecule.

234 A second important outcome of the tribological AIMD simulations concerns the reaction  
 235 products. As observed under extreme confinement, the final products of TMPi dissociation are CO  
 236 molecules and atomic P. This simple observation accompanied by the evidence we provide on the  
 237 effects of P in reducing the adhesion and increasing the metal separation is sufficient to uncover the  
 238 mechanisms underlying the friction reduction observed in GPL by TMPi. Our results show, in fact,  
 239 that in boundary lubrication conditions elemental O and C atoms are not released from TMPi  
 240 because these two atoms remain bounded in the CO molecule, which does not dissociate on iron [39]  
 241 and can desorb from the interface. H atoms can desorb as well in the form of H<sub>2</sub> or diffuse into the  
 242 iron bulk. Therefore what remains at the interface after TMPi decomposition is elemental P, as  
 243 clearly identified by XPS analysis performed *in situ* after the GPL experiment.[16] Iron phosphide  
 244 presents low friction, as evidenced by the experiment and in first principles calculations.[21] While a  
 245 similar lubricating effect can be provided by sulfur,[40] and graphene [41-43] it is not provided by  
 246 atomic oxygen.[21] The AIMD simulations reveal that O adsorption does not compete with P  
 247 adsorption during TMPi decomposition. This explain the higher efficiency of phosphites than  
 248 phosphates, where an extra oxygen per molecule is present, in reducing friction observed in the  
 249 experiments.[21] It is important to notice that the presence of iron oxide on the surface could alter  
 250 the dissociation path, e.g. in aryl phosphates and phosphites there is evidence that the C-O bond  
 251 cleavage is more likely than the P-O bond.

252 A recent first principles study of P chemisorption [44] revealed that by increasing the P  
 253 coverage on the Fe(110) surface, the lateral interaction among the adsorbates increases. This in-plane  
 254 interaction is responsible for the decrease of adhesion observed when two P-covered surfaces are  
 255 brought into contact. The next step in our analysis of the tribochemistry of organophosphorus  
 256 additives will be to consider a larger amount of additive molecules in our supercell to monitor in real  
 257 time the formation and the effects of iron phosphide at higher concentration of P. Such simulation  
 258 requires enlarging the size of the simulated system, with consequent increase of the computational  
 259 cost of AIMD. Hybrid quantum-mechanics/molecular-mechanics (QM/MM) technique, recently

260 applied for the first time to tribology by our group,[45] will allow us to face this computational  
261 challenge.  
262

## 263 5. Conclusions

264 The potential of *ab initio* molecular dynamics in the research on lubricant materials has been  
265 highlighted through the study of the tribochemistry of a model organophosphorus additive. GPL  
266 experiment and spectroscopic analysis revealed that the ability of phosphite additives to reduce  
267 friction relies on the formation of an iron phosphide tribofilm. *Ab initio* molecular dynamics of TMPi  
268 molecules at sliding iron interfaces uncovered the atomistic mechanisms that lead to P release in  
269 boundary lubrication conditions. Such understanding can explain the different functionalities of  
270 phosphite and phosphates additives. Moreover, the activation time for molecular dissociation  
271 observed in our tribological simulations turned out to be order of magnitudes smaller than that  
272 expected at the open surface in static conditions on the basis of the calculated activation barriers.  
273 This observation and the observed dependence of reaction rates on the applied load constitute a  
274 clear evidence that mechanical stress are able to active reactions even at room temperature.

275 **Supplementary Materials:** The following are available online at [www.mdpi.com/link](http://www.mdpi.com/link), Video S1: AIMD  
276 simulation of TMPi tribochemistry at 500 MPa load; Video S2: AIMD simulation of TMPi tribochemistry at 2  
277 GPa load; Video S3: AIMD simulation of TMPi tribochemistry at 5 GPa load.

278 **Acknowledgments:** This work was partially supported by the University of Modena and Reggio Emilia  
279 through the FAR project. M. C. Righi acknowledges support by the European Union through the MAX Centre  
280 of Excellence (Grant No. 676598). The authors thankfully acknowledge CINECA for super-computing resource  
281 through the project ISCRA B StressRx. Several pictures in this letter were created with the help of XCrySDen  
282 [46].

283 **Conflicts of Interest:** "The authors declare no conflict of interest."

## 284 References

- 285 1. H. Spikes, *Tribol. Lett.*, 2015, 60(5), 1–26.
- 286 2. Z. Tang and S. Li, *Curr. Opin. Solid State Mater. Sci.*, 2014, 18, 119.
- 287 3. H. Spikes, *Lubr. Sci.*, 2008, 20, 103.
- 288 4. J. Van Rensselar, *Power Transmission Engineering*, 2003.
- 289 5. A. Erdemir, G. Ramirez, O. Eryilmaz, B. Narayanan, Y. Liao, G. Kamath, SK. Sankaranarayanan, *Nature*  
290 2016, 4;536(7614):67-71
- 291 6. J.P. Ewen, M. Heyes, D. Dini, *Friction* 2018, DOI/10.1007/s40544.018-0207-9
- 292 7. S. Matsui and H. Komatsubara, US20070287643, Nippon Oil Corporation, 2007.
- 293 8. T. Craig and T. Thomas, WO2007111741, Lubrizol Corporation, 2007.
- 294 9. O. Furlong and F. Gao, *Tribol. Int.*, 2008, 40, 699.
- 295 10. A. Riga, J. Cahoon and W. R. Pistillo, *Tribol. Lett.*, 2000, 9, 219.
- 296 11. F. Gao, P. V. Kotvis, D. Stacchiola and W. T. Tysoe, *Tribol. Lett.*, 2005, 18, 377.
- 297 12. F. Gao, O. Furlong, P. V. Kotvis and W. T. Tysoe, *Langmuir*, 2004, 20, 7557.
- 298 13. D. Philippon, et al., *Tribol. Int.*, 2011, 44, 113.
- 299 14. D. Philippon, et al., *Tribol. Mater., Surf. Interfaces*, 2007, 1, 113.
- 300 15. D. Philippon, et al., *Thin Solid Films*, 2012, 524, 191.
- 301 16. M. C. Righi, S. Loehl' e, M. I. De Barros-Bouchet, D. Philippon and J. M. Martin, *RSC Adv.*, 2015, 5, 101162.
- 302 17. P. Giannozi, et al., *J. Phys.: Condens. Matter*, 2009, 21, 395502.
- 303 18. J. P. Perdew, K. Burke and M. Ernzerhof, *Phys. Rev. Lett.*, 1996, 77, 3865.
- 304 19. P. Blonski and A. Kiejna, *Surf. Sci.*, 2007, 601, 123.
- 305 20. Monkhorst HJ, Pack JD. *Phys Rev B*. 1976, 13, 5188.
- 306 21. M. I. De Barros-Bouchet et al. *RSC Adv.*, 2015, 5, 49270
- 307 22. A. W. Holbert, A. Batteas, A. Wong-Foy, T. S. Rufael and C. M. Friend, *Surf. Sci.*, 1998, 401, L437–L443.
- 308 23. G. Henkelman, B. P. Uberuaga and H. J. Jonsson, *J. Chem. Phys.*, 2000, 113, 9978.
- 309 24. Zilibotti G, Corni S, Righi MC. *Phys Rev Lett*. 2013, 111, 146101.

- 310 25. Kajita S, Righi MC. *Carbon*. 2016,103, 193.
- 311 26. Fischer TE. *Ann Rev Mater Sci*. 1988;18, 303.
- 312 27. Heinicke G. *Tribochemistry*. Munchen: Carl Hanser Verlag; 1984.
- 313 28. Thiessen PA, Meyer K, Heinicke G. *Grundlagen der Tribochemie*. Berlin: Akademie Verlag; 1967.
- 314 29. Gosvami NN et al. *Science*. 201, 348, 102.
- 315 30. Gotsmann B, Lantz MA. *Phys Rev Lett*. 2008, 101, 125501.
- 316 31. Hickenboth CR et al. *Nature*. 2007, 446, 423.
- 317 32. Furlong OJ et al. *ACS Appl Mater Interf*. 2011, 3, 795.
- 318 33. Furlong OJ et al. *RSC Adv*. 2014, 4, 24059.
- 319 34. Ghanbarzadeh A et al. *Tribol Lett*. 2016, 1, 61.
- 320 35. Felts JR et al. *Nat Commun*. 2015, 6, 6467.
- 321 36. Jacobs DB, Carpick RW. *Nat Nanotechnol*. 2013, 8, 108.
- 322 37. Adams HL, Garvey MT, Ramasamy SU, Ye Z, Martini A, Tysoe WT, *J Phys Chem C*. 2015,119, 7115.
- 323 38. Zhang J, Spikes H., *Tribol Lett*. 2016, 63, 24.
- 324 39. D.E. Jiang, et al. *Surf. Sci*. 2004, 570,167.
- 325 40. M. C. Righi et al., *RSC Adv*., 2016, 6, 47753.
- 326 41. P. Restuccia and M. Righi, *Carbon* 106, 118 (2016).
- 327 42. D. Marchetto, P. Restuccia, A. Ballestrazzi, M. C. Righi, A. Rota and S. Valeri, *Carbon* 116, 375 (2017).
- 328 43. G. Levita, P. Restuccia, and M. C. Righi, *Carbon* 107 (2016) 878.
- 329 44. G. Fatti, P. Restuccia, S. Lohele', C. Calandra and M. C. Righi, to be published
- 330 45. P. Restuccia, M. Ferrario and M. C. Righi, to be published
- 331 46. Kokalj, *Computational Materials Science* 28, 155 (2003), proceedings of the Symposium on Software De-
- 332 velopment for Process and Materials Design.
- 333
- 334